



## OPEN ACCESS

## EDITED BY

Edwin Roger Parra,  
University of Texas MD Anderson  
Cancer Center, United States

## REVIEWED BY

Milos Milovancevic,  
Masinski Fakultet - Univerziteta U  
Nisu, Serbia  
Baohua Sun,  
University of Texas MD Anderson  
Cancer Center, United States

## \*CORRESPONDENCE

Pinghua Tu  
tupinghua@126.com  
Zhanling Wu  
1046923032@qq.com

## SPECIALTY SECTION

This article was submitted to  
Thoracic Oncology,  
a section of the journal  
Frontiers in Oncology

RECEIVED 25 February 2022

ACCEPTED 29 August 2022

PUBLISHED 11 October 2022

## CITATION

Tu P, Li X, Cao L, Zhong M, Xie Z and  
Wu Z (2022) Machine learning and BP  
neural network revealed abnormal B  
cell infiltration predicts the survival of  
lung cancer patients.  
*Front. Oncol.* 12:882018.  
doi: 10.3389/fonc.2022.882018

## COPYRIGHT

© 2022 Tu, Li, Cao, Zhong, Xie and Wu.  
This is an open-access article  
distributed under the terms of the  
[Creative Commons Attribution License  
\(CC BY\)](https://creativecommons.org/licenses/by/4.0/). The use, distribution or  
reproduction in other forums is  
permitted, provided the original  
author(s) and the copyright owner(s)  
are credited and that the original  
publication in this journal is cited, in  
accordance with accepted academic  
practice. No use, distribution or  
reproduction is permitted which does  
not comply with these terms.

# Machine learning and BP neural network revealed abnormal B cell infiltration predicts the survival of lung cancer patients

Pinghua Tu\*, Xinjun Li, Lingli Cao, Minghua Zhong,  
Zhibin Xie and Zhanling Wu\*

Department of Respiratory and Critical Care Medicine, Xiaogan Hospital Affiliated to Wuhan University of Science and Technology, Xiaogan City, China

FAM83A gene is related to the invasion and metastasis of various tumors. However, the abnormal immune cell infiltration associated with the gene is poorly understood in the pathogenesis and prognosis of NSCLC. Based on the TCGA and GEO databases, we used COX regression and machine learning algorithms (CIBERSORT, random forest, and back propagation neural network) to study the prognostic value of FAM83A and immune infiltration characteristics in NSCLC. High FAM83A expression was significantly associated with poor prognosis of NSCLC patients ( $p = 0.00016$ ), and had excellent prognostic independence. At the same time, the expression level of FAM83A is significantly related to the T, N, and Stage. Subsequently, based on machine learning strategies, we found that the infiltration level of naive B cells was negatively correlated with the expression of FAM83A. The low infiltration of naive B cells was significantly related to the poor overall survival rate of NSCLC ( $p = 0.0072$ ). In addition, Cox regression confirmed that FAM83A and naive B cells are risk factors for the prognosis of NSCLC patients. The nomogram combining FAM83A and naive B cells (C-index = 0.748) has a more accurate prognostic ability than the Stage (C-index = 0.651) system. Our analysis shows that abnormal infiltration of naive B cells associated with FAM83A is a key factor in the prognostic prediction of NSCLC patients.

## KEYWORDS

random forest, back propagation (BP) neural network, COX regression, prognostic prediction, immune infiltration

**Abbreviations:** AUC, area under curve; BP, back propagation neural network; EGFR-TKI, epidermal growth factor receptor-tyrosine kinase inhibitor; FAM83A, family with sequence similarity 83 member A; GEO, gene expression omnibus; K-M, Kaplan-Meier; LASSO, least absolute shrinkage and selection operator; LUAD, lung adenocarcinoma; LUSC, lung squamous cell carcinoma; MSE, mean square error; NSCLC, non-small cell lung cancer; RF, random forest; ROC, receiver operating characteristic; SVM, support vector machine; TCGA, the cancer genome atlas; Tfh, T cells follicular helper; Tregs, T cells regulatory.

## Introduction

Lung cancer is a common malignant tumor in clinical practice in the respiratory system, with high morbidity and mortality. Non-small cell lung cancer (NSCLC) accounts for around 80% to 85% of all lung cancer cases. (1). Currently, distant metastasis and recurrence are still a severe challenge to NSCLC undergoing surgery (2). Targeted drugs and immunotherapy have opened a new era of NSCLC treatment (3). However, only a fraction of patients benefit from immunotherapy (4). In addition, current prognostic biomarkers are insufficient to accurately assess NSCLC patients' prognosis due to tumor cell heterogeneity and drug resistance (4, 5). As a result, developing potent and precise prognostic biomarkers is critical for improving NSCLC prognosis and tailored treatment.

On chromosome 8q24, the family with sequence similarity 83 member A (FAM83A) gene, is found. Initially, the authors identified FAM83A as a potential oncogenic gene through bioinformatics methods. Previous studies reported that FAM83A plays a role in promoting cancer in a variety of tumors (6). Lee et al. (7) revealed that FAM83A overexpression induced resistance to epidermal growth factor receptor-tyrosine kinase inhibitor (EGFR-TKI), leading to the breast cancer patients' poor prognosis (8). Recently, Hu et al. (9) found that FAM83A may promote NSCLC tumorigenesis through the ERK and PI3K/Akt/mTOR pathways. However, studies have found that FAM83 family genes maybe a risk factor for the NSCLC patients survival (10). However, the abnormal infiltration of immune cells associated with FAM83A is poorly understood in the pathogenesis and prognosis of NSCLC. Studying the FAM83A immune infiltration may guide the treatment and prognosis of NSCLC.

The widely used machine learning algorithms enable analyzing large population gene sequencing or microarray data from a new perspective. Machine learning algorithms, including random forest, least absolute shrinkage and selection operator (LASSO), and the bio-inspired algorithm, back propagation neural network (BPNN) can avoid the risk of overfitting. And the biomarkers defined by machine learning algorithms have shown better performance in prognostic prediction than those developed through traditional statistical methods in the past decades (11). Therefore, the machine learning algorithms identified a biomarker related to the prognosis and immune infiltration of NSCLC.

The study first comprehensively analyzed the expression level, prognostic performance, and clinical relevance of FAM83A in NSCLC. Subsequently, we tested the prognostic independence of FAM83A. Next, we applied CIBERSORT deconvolution algorithm to determine immune cell infiltration in the NSCLC microenvironment. Finally, we used LASSO, random forest (RF) and BPNN algorithms to identify immune cells with abnormal infiltration associated with FAM83A.

## Materials and methods

### Data source

The cancer genome atlas (TCGA, <https://cancergenome.nih.gov>) database was used to download lung adenocarcinoma (LUAD) and lung squamous cell carcinoma (LUSC) expression data as well as clinical follow-up data. Then we kept the expression matrix of 20,531 genes containing 110 normal and 1019 tumor samples. At the same time, the mRNA expression of GSE37745 containing 196 samples and the corresponding clinical data are downloaded from the gene expression omnibus (GEO, <https://www.ncbi.nlm.nih.gov/geo/>) database. Finally, we normalized data and eliminated patients with a survival time  $\leq 0$  months.

### CIBERSORT analysis

We used the support vector machine (SVM) based CIBERSORT deconvolution algorithm to investigate the heterogeneity in the tumor immune microenvironment (12). Subsequently, we run 1000 permutations through the LM22 gene signature file to evaluate 22 immune cells' infiltration scores.

### LASSO analysis

Based on FAM83A expression grouping (group by median), we used LASSO analysis to screen key immune cells from 22 immune cells. LASSO applied the L1 norm to punish the model for achieving constraints on the objective function (13).

The complexity of the model is controlled by  $\lambda$ . Specifically, the penalty of the linear model is positively correlated with  $\lambda$ . In this study, when we call `rng(seed)` to generate random numbers, the numbers generated each time are random. However, when we call and set the seed value in advance, the random number generated by `rng(seed)` will be the same.

### Random forest analysis

The main idea of random forest (RF) is to obtain a series of decision trees (14). The algorithm captures complex interactions to get a set of average features. The study uses the "randomForest" package to implement the training: (1) extract patient samples from the training data set TCGA as a random subset (2) use a random subset of predictors to grow each tree. Tree branches grow to the maximum without pruning. (3) Repeat the second step until the number of branches has increased to the set value. Then we average the predicted results.

## Back propagation neural network analysis

The LASSO-RF overlapping immune cells were included in the multivariate COX analysis to identify significant candidate features. Subsequently, the candidate features are reversely verified through the artificial neural network function input. BPNN is a hierarchical neural network consisting of the input, hidden, and output layer. The algorithm continuously adjusts the network model parameters by back-propagating the calculation error and correcting it simultaneously to maintain a one-to-one correspondence close to the target. BPNN aims to iteratively change the weights between neurons to minimize the error, defined as the squared difference between the expected and actual results of the output node, summed over the training pattern (training dataset) output neuron. BPNN reduces the error between the predicted result and the true output by changing the weight.

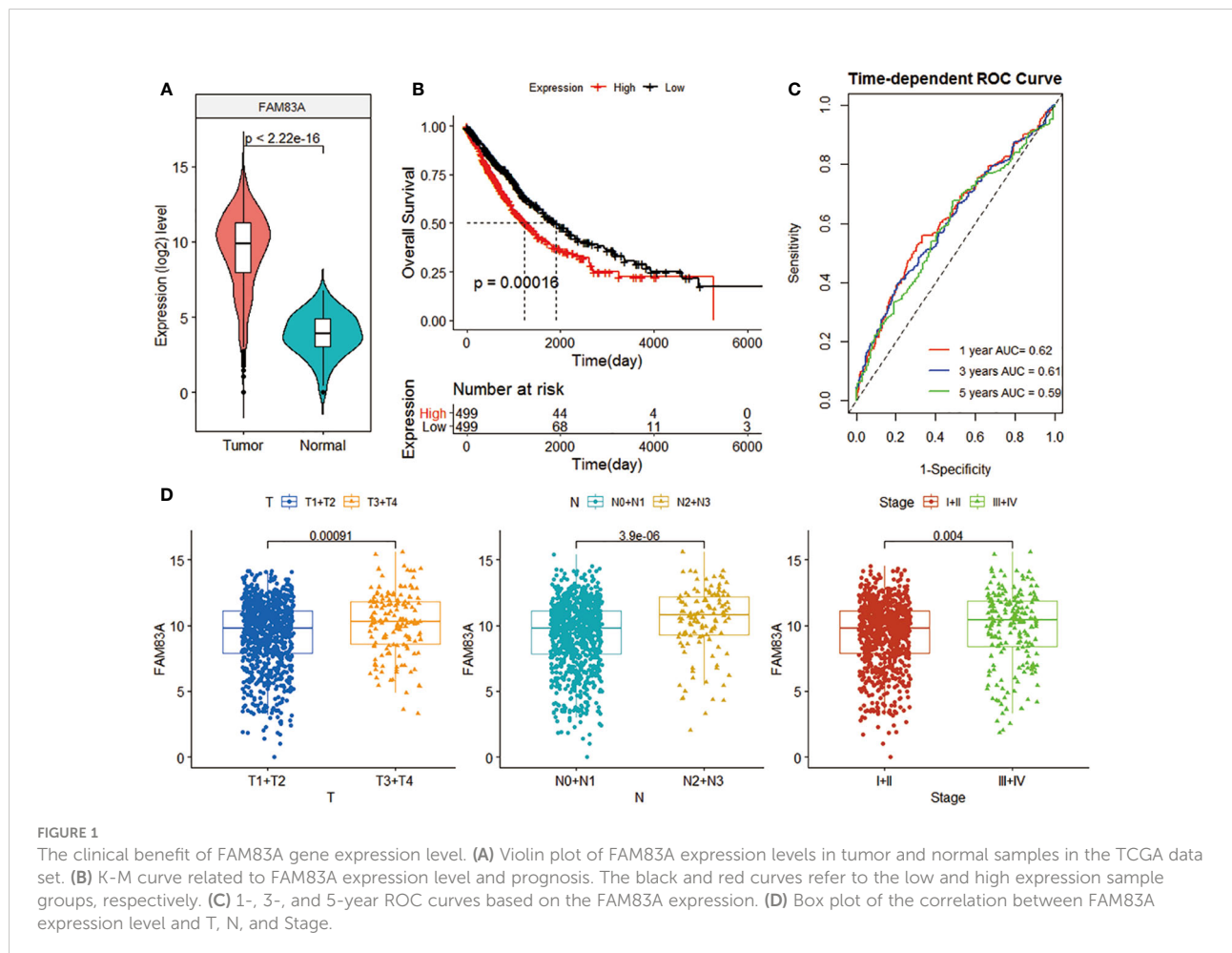
## Statistical analysis

The study performed bioinformatics analysis using R v3.6.1 environment.  $p < 0.05$  was considered statistically significant. The regression of K-M and COX relies on the “survival v3.2-3” package. The tROC (time-dependent receiver operating characteristic) and LASSO algorithms are implemented by “timeROC v 0.4” and “glmnet v4.0-2” respectively.

## Results

### Clinical manifestations of FAM83A

FAM83A expression in NSCLC was significantly higher than in normal tissues ( $p < 2.22e-16$ ; Figure 1A). The Kaplan-Meier curve, time-dependent ROC curve, T, N, Stage confirmed the clinical performance of FAM83A (Figures 1B–D). The survival



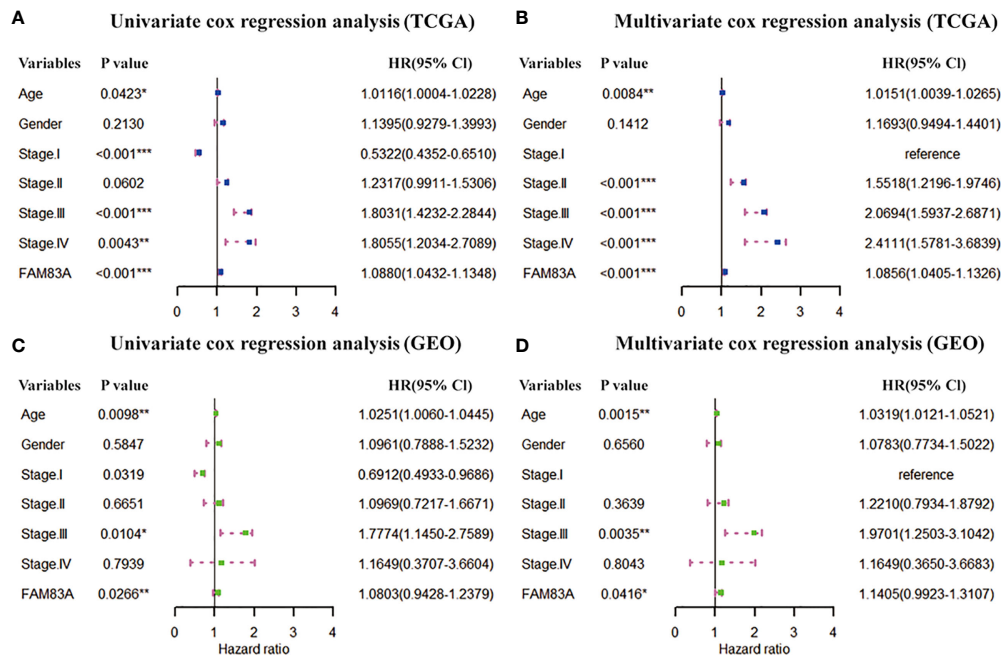


**FIGURE 2** Prognostic independence of FAM83A based on TCGA and GEO datasets. (A) Univariate and (B) multivariate COX forest plot of FAM83A gene and clinical factors based on the TCGA data set. (C) Univariate and (D) multivariate COX forest plots of FAM83A and clinical factors based on GEO dataset. (\*p<0.05, \*\*p<0.01, \*\*\*p<0.001).

analysis found that low FAM83A expression substantially improves the patient’s survival (p = 0.00016; Figure 2B). In addition, tROC showed that the 1, 3, and 5-year area under curve (AUC) values expressed by FAM83A were 0.62, 0.61, and 0.59, respectively (Figure 3C). Figure 4D shows that the expression level of FAM83A in the later stages of T (p = 0.00091), N (p = 3.9e-06) and Stage (p = 0.004) was significantly higher than in the early stage.

### The independent prognostic value of FAM83A

The clinical information (age, gender and stage) and FAM83A were included in the Cox regression to estimate the independent prognostic value of FAM83A. Univariate COX regression in the TCGA dataset showed FAM83A (HR = 1.0880, p < 0.001), Age (HR = 1.0116, p = 0.0423) and Stage (stage I, HR = 0.5322, p < 0.001; stage III, HR = 1.8031, p < 0.001; stage IV, HR = 1.8055, p = 0.0043) are prognostic risk factors for NSCLC (Figure 2A). The multivariate Cox regression found that FAM83A (HR=1.0856, p < 0.001), Age (HR=1.0151, p = 0.0084) and stage (stage II, HR = 1.5518, p < 0.001; stage III, HR = 2.0694, p < 0.001; stage IV, HR = 2.4111, p < 0.001) is an independent marker for assessing the survival

of NSCLC (Figure 2B). Similarly, the GSE37745 dataset further confirmed the prognostic independence of FAM83A (Figures 2C, D).

### Immune cell infiltration

The CIBERSORT deconvolution algorithm obtains the percentage of infiltration of 22 immune cells in each NSCLC sample. We found that macrophages M2, M0, and T cells CD4 memory resting accounted for a larger proportion (Figure 3A). Subsequently, we took the arithmetic mean of the immune cell infiltration rate of 998 NSCLC samples as its infiltration rate in the FAM83A high expression group and low expression group. Each immune cell subtype’s infiltration ratio is the ratio of its population to the total number of 22 immune cells in the immunological microenvironment. The top 5 immune cell subtypes with the highest penetration rate in the FAM83A high expression group are macrophages M2 (20.00%), macrophages M0 (17.93%), T cells CD4 memory resting (12.13%), T cells follicular helper (Tfh) (7.65%), and plasma cells (6.20%) (Figure 3B). The top five immune cell subtypes with the highest infiltration rate in the FAM83A low expression group were macrophages M2 (19.40%), macrophages M0 (17.63%), T cells CD4 memory resting (12.03%), Tfh (7.96%) and plasma cells



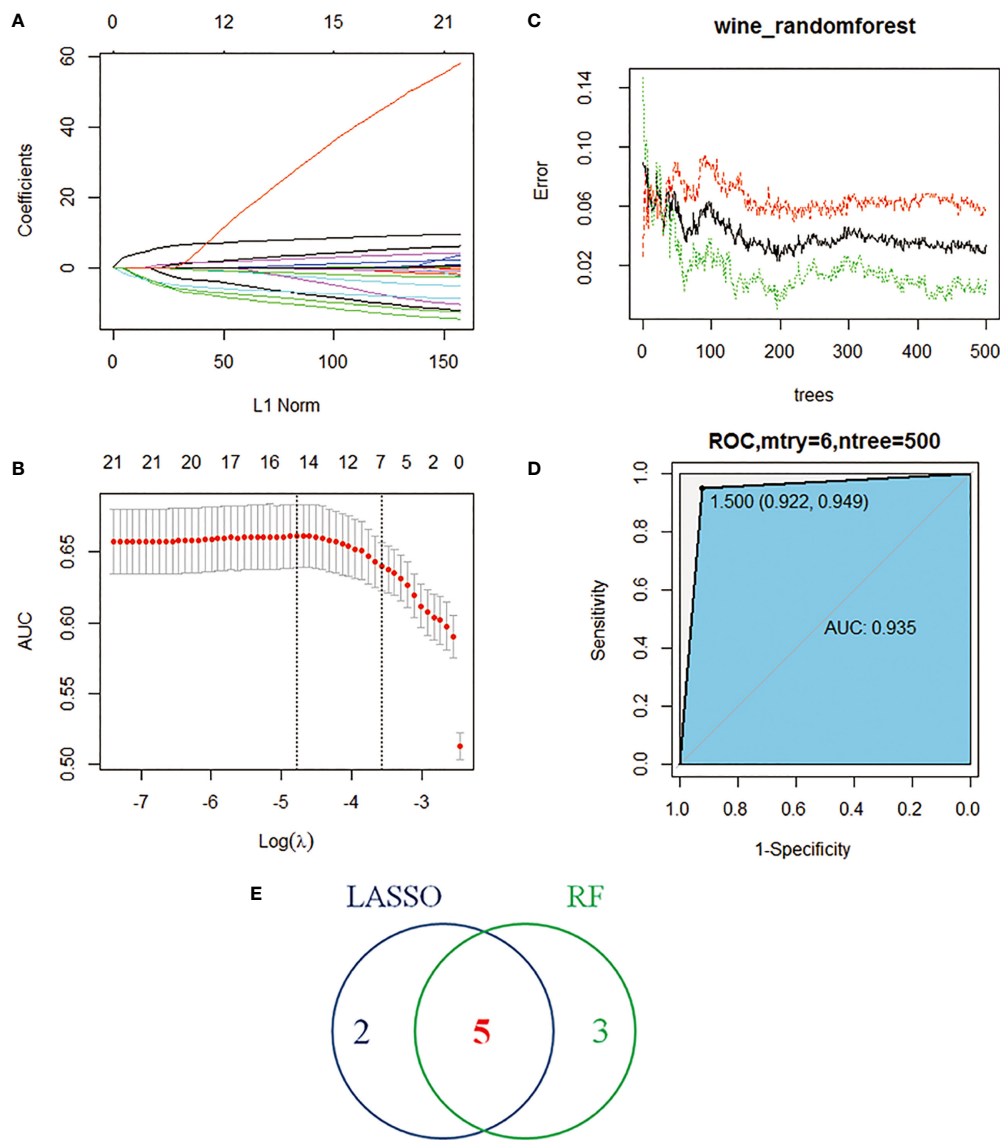


**FIGURE 4** Machine learning identifies key immune cells. **(A)** Distribution of LASSO coefficients for 22 immune cells. **(B)** Penalty plot of 22 immune cells in the LASSO model, error bars represent standard error. **(C)** the error variation of the RF algorithm, red and green represent the error rate of high and low FAM83A expression groups, and black represents the overflow error rate. **(D)** Random forest analysis results **(E)** Five immune cell types identified by LASSO and RF algorithms.

cells CD4 memory activated, Tfh, dendritic cells activated and neutrophils (Table 1). RF analysis obtained 8 key immune cells (Figure 4C), namely naive B cells, Tregs, T cells CD4 memory resting, macrophages M1, macrophages M2, neutrophils, Tfh and dendritic cells activated (Table 2). At the same time, the AUCs of the RF model is 0.935 (Figure 4D). Figure 4E identifies five overlapping immune cells (naive B cells, Tregs, Tfh, dendritic cells activated and neutrophils).

### Identification of candidate features

FAM83A expression is negatively correlated with naive B.cells. (Cor = -0.20) and Tfh (Cor = -0.07), and significantly positively correlated with DCs activated (Cor = 0.17), Tregs (Cor = 0.09) and neutrophils (Cor = 0.14) (Figure 5A). We further included five immune characteristics in the multivariate COX regression. The results showed that naive

TABLE 1 LASSO analysis of 7 candidate immune cells.

Immune cells	LASSO Coefficient
B cells naive	1.6275
T cells regulatory (Tregs)	-0.9268
B cells memory	1.3139
T cells CD4 memory activated	-0.2186
Dendritic cells activated	-1.9478
Neutrophils	-0.6484
T cells follicular helper	-1.6101

TABLE 2 RF analysis of 8 candidate immune cells.

Immune cells	MeanDecreaseGini
B cells naive	36.7805
T cells regulatory (Tregs)	36.1051
T.cells CD4 memory resting	34.2748
Macrophages M1	32.4069
Macrophages M2	31.6643
Neutrophils	31.6200
T cells follicular helper	30.5608
Dendritic cells activated	29.3928

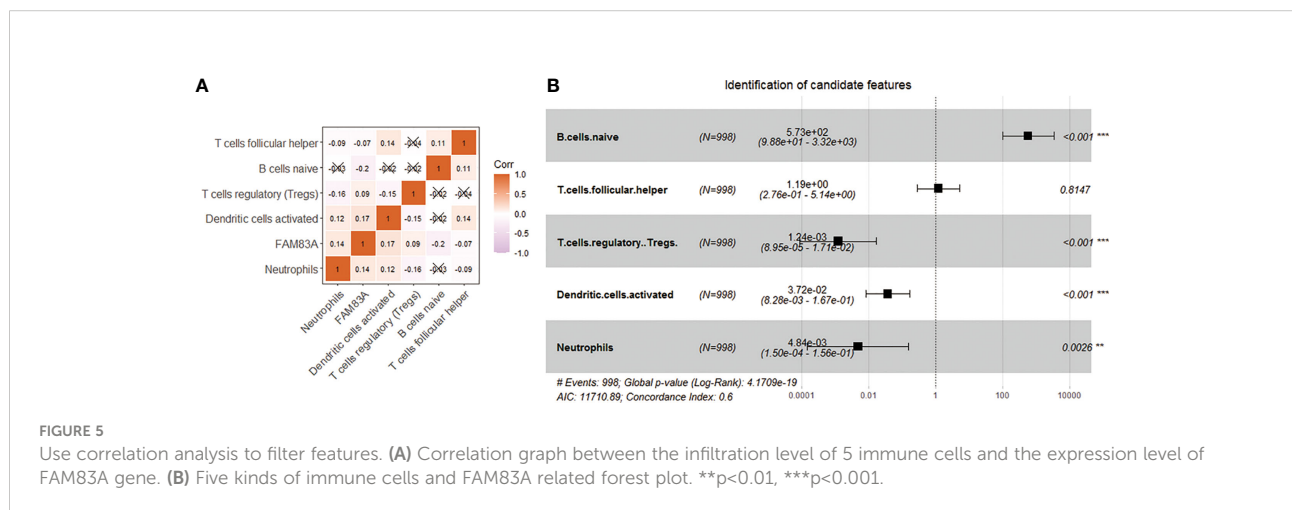
B cells ( $p < 0.001$ ), Tregs ( $p < 0.001$ ), dendritic cells activated ( $p < 0.001$ ) and neutrophils ( $p = 0.0026$ ) are the key immune landscapes associated with FAM83A (Figure 5B). Therefore, FAM83A associated 4 types of immune cells served as candidate features.

### BPNN verification

We use candidate features as the input of BPNN to further verify the machine learning results. The number of hidden layers set by BPNN is 2, and the number of nodes is 10. The FAM83A expression acted as the output of the algorithm. 70% of the data served as the training data set, and the other 30% validates and tests the neural network. The study executed the algorithm based on mean square error (MSE). The result proves that the MSE is 0.00043915, and the best performance of the BPNN model appeared at 5 epochs (Figure 6A). Figure 6B shows that the prediction error range is -0.01916 to 0.02515. In addition, we also found that the training set ( $R = 0.97884$ ), the validation set ( $R = 0.99853$ ), and the test set ( $R = 0.99755$ ) have high regression values (Figure 6C), indicating a small prediction bias of the BPNN model. These results suggest that the candidate features are significantly related to FAM83A expression.

### Immune cells associated with FAM83A

The study further investigates the prognostic ability of immune cells associated with FAM83A. We performed K-M analysis on FAM83A associated immune cells and found that the low infiltration of naive B cells was significantly associated with the poor prognosis of NSCLC patients ( $p = 0.0072$ ; Figure 7A). However, Tregs, dendritic cells activated and neutrophils have no correlation with the overall survival of NSCLC patients (Figure S1). Naive B cells infiltration in the low expression group was significantly higher than in the FAM83A high expression group ( $p = 6.2e-08$ ; Figure 7B). Figure 7C shows that the naive B cells infiltration is significantly



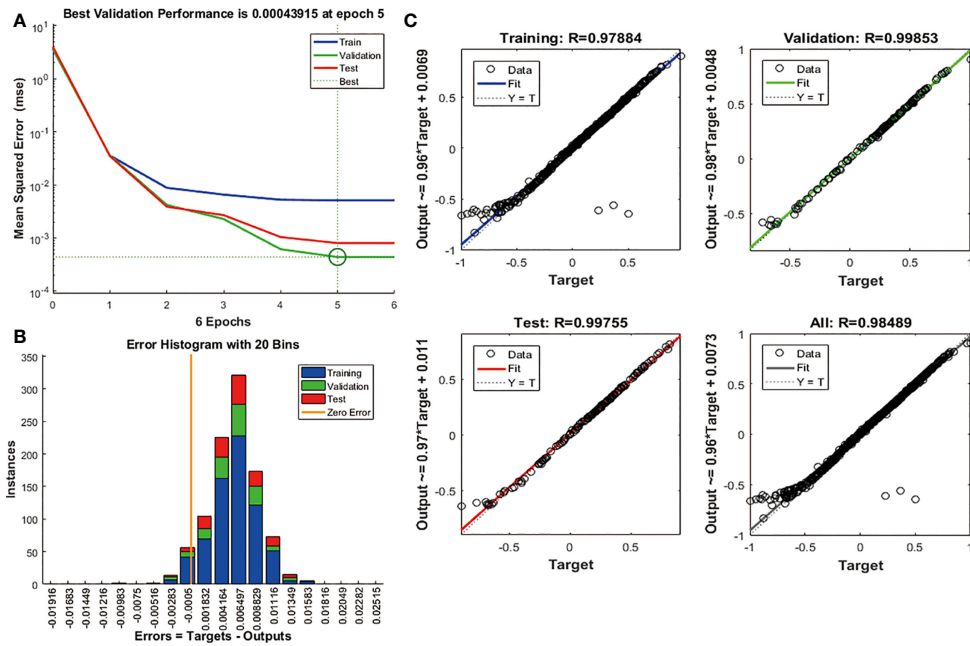


**FIGURE 6** Validation of candidate features based on BPNN algorithm. **(A)** The change curve of MSE and epochs of the BPNN model. **(B)** The error distribution bar graph of the BPNN model. **(C)** Linear regression graph of BPNN model.

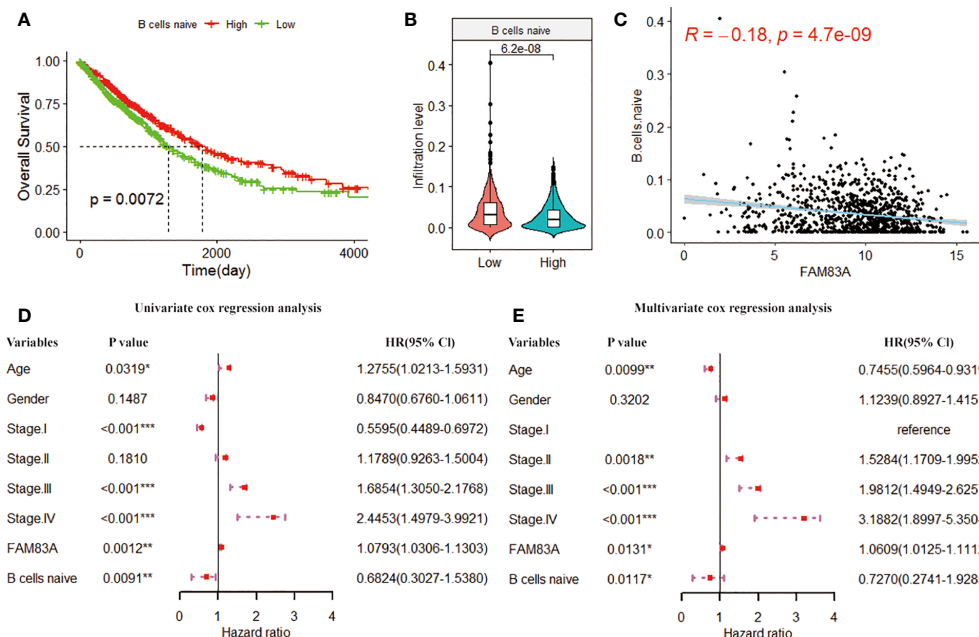


**FIGURE 7** The K-M curve of **(A)** naive B cells infiltration level and overall survival. The green and red curves represent the sample group with low expression and high infiltration level, respectively. **(B)** Violin plot of naive B cell infiltration in FAM83A high and low expression groups. **(C)** Scatter plot of the correlation between the infiltration level of naive B cells and the FAM83A expression. **(D)** Univariate cox forest plots related to the prognosis of clinical factors. **(E)** Multivariate cox forest plots related to the prognosis of clinical factors. (\*p<0.05, \*\*p<0.01, \*\*\*p<0.001).

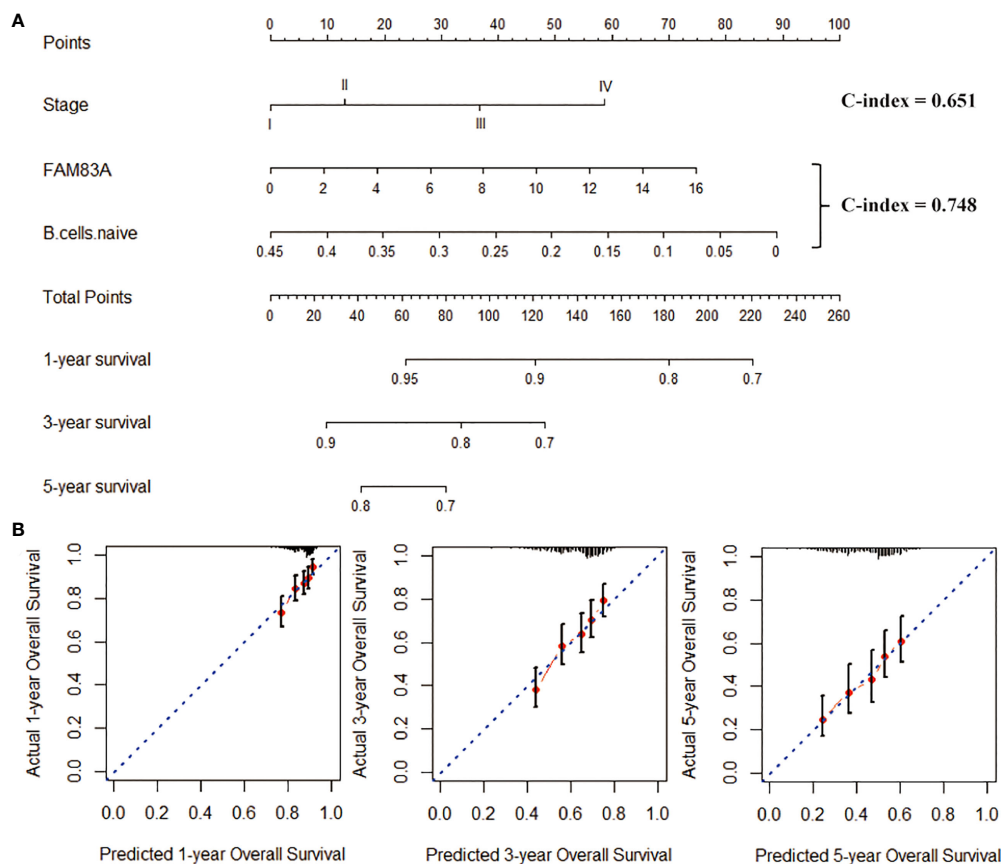


FIGURE 8

Construction of the nomogram graph. (A) Stage, FAM83A and naive B cells survival rate prediction model nomogram. (B) The nomogram is a line graph of the consistency between the predicted and actual survival rates of 1-, 3-, and 5-year survival rates. The horizontal and the vertical axis represents the predicted and the actual survival rate, respectively.

correlated with the FAM83A expression ( $Cor = -0.18, p = 4.7e-09$ ). Then we included naive B cells, FAM83A and clinical information into the Cox regression analysis after excluding samples with an immune score of 0. Univariate and multivariate analysis showed that FAM83A and naive B cells are risk factors for the prognosis of NSCLC ( $p < 0.05$ , Figure 7D, E). Therefore, we confirmed that the abnormal infiltration of naive B cells associated with FAM83A is a key factor in predicting the prognosis of NSCLC patients.

## Nomogram analysis

We included naive B cells and FAM83A in the nomogram construction due to the excellent prognostic ability. The nomogram created by combining naive B cells and FAM83A (C-index = 0.748; Figure 8A) has better prognostic predictive ability than Stage (C-index = 0.651). And the nomogram matches the best prediction performance (Figure 8B).

## Discussion

The 5-year survival rate of advanced NSCLC is 5-15% (15). As immunotherapy has made significant breakthroughs in NSCLC, the human immune system recruits and activates T cells to recognize and eliminate cancer cells (16). However, not every patient responds to this treatment. Therefore, clarifying and finding new immune-related therapeutic targets may provide more clues for targeted therapy of NSCLC. Studies have found (17, 18) that FAM83 family members A, B, and D have carcinogenic potential. The expression of FAM83A is also related to the growth rate of tumors. The expression of the endogenous FAM83A and the increase in DNA copy number make the surviving tumor cells resistant to treatment (19).

FAM83 family genes activate the MEK/ERK signaling pathway to affect the occurrence and development of tumors (20). FAM83A has long been identified as a tumor-

specific biomarker and is highly expressed in nearly half of lung cancer tissue samples. FAM83A promotes the progression of NSCLC through ERK and PI3K/Akt/mTOR signaling pathways (9). Zheng et al. (21) found that FAM83A enhances the proliferation and invasion of NSCLC cells by modulating the Wnt and Hippo signaling pathways, as well as the EMT process. FAM83A is highly expressed in NSCLC, related to advanced TNM staging and poor prognosis, consistent with the study. The study analyzed the relationship between the FAM83A expression and the prognosis, survival rate, tumor stage, and lymph node metastasis of NSCLC patients through TCGA data. NSCLC patients with high FAM83A expression have a low survival rate that is significantly related to lymph node metastases and NSCLC clinical stage. Zhang et al. (22) proved that the FAM83A expression in advanced NSCLC tumors (stages  $\alpha$  to  $\alpha$ ) is higher than that in early stage NSCLC tumors (stages  $\alpha$  to  $\alpha$ ). This is consistent with the significant correlation between the FAM83A expression and the NSCLC stage in this study. The above analysis suggests that FAM83A may be a prognostic biomarker for NSCLC.

We evaluated the level of immune cell infiltration based on the CIBERSORT algorithm. Among them, macrophages M2, macrophages M0 and T cells CD4 memory resting accounted for a relatively large proportion of NSCLC. Macrophages are highly varied and can be classified into M1 and M2 subtypes as they progress from the M0 stage, through local microenvironmental stimulation (23). Macrophages M2 suppressed inflammation and reduced the body's immune response by secreting inhibitors to promote tumor metastasis (24). In addition, Jin et al. (25) found that the heterogeneity of immunotherapy in NSCLC patients was significantly associated with abnormal infiltration of T cells CD4 memory resting.

The LASSO and RF algorithms helped us identify five immune infiltrating cells significantly related to NSCLC patients. Studies have found that the expansion of Tregs hinders tumor immunotherapy, leading to immunotherapy failure (26). Furthermore, studies have found high Tregs infiltration is associated with poor prognosis of NSCLC patients (27, 28). Guo et al. (29) confirmed that the infiltration rate of Tfh in advanced-stage patients is higher than that in early-stage patients. Tfh may be an important prognostic biomarker for evaluating the adverse clinical outcome of NSCLC patients (30). Li et al. (31) found that DCs activated immunotherapy has a good effect on treating non-small cell lung cancer. In addition, neutrophil content can predict lymphocyte depletion and failure of anti-PD-1 therapy in NSCLC (32).

The LASSO algorithm has the function of dimensionality reduction, which can directly reduce the number of features and

make the feature selection. When the features have strong semantics, it is better to use LASSO, and the subsequent analysis will be more interpretable. The random forest is an ensemble learning algorithm that can calculate the features that contribute the most to the final result. BPNN can combine data, and the final result is an inexplicable model that can only realize input data and make predictions. Therefore, the combination of LASSO, random forest, and BPNN can reasonably achieve a comprehensive dimensionality reduction, feature selection, and interpretability analysis.

Cox regression, BPNN algorithm and K-M analysis demonstrated that the naive B cells' low infiltration was significantly related to the poor prognosis of NSCLC patients, confirmed by Chen et al. (33). Naive B cells participated in the immunosuppressive process and promoted the development of lung cancer (34). Mechanism 1: the high infiltration of naive B cells promotes the immune activity of patients with lung cancer (35). Mechanism 2: naive B cells with low infiltration in the lung cancer microenvironment directly promotes the proliferation of lung cancer cells (36). In addition, we confirmed that the naive B cells infiltration was negatively correlated with the FAM83A expression. At the same time, FAM83A and naive B cells are independent risk factors for the prognosis of NSCLC patients. Therefore, abnormal infiltration of naive B cells associated with FAM83A is a key factor in predicting the NSCLC patients' prognosis.

Compared with other clinical features, FAM83A and naive B cells showed good prognostic independence. Interestingly, Cox regression analysis shows the powerful predictive ability of stage. The stage provided effective prognostic diagnosis and appropriate treatment guidance (37). FAM83A and naive B cells prognostic characteristics (C-index = 0.748) have more advantages in survival prediction than Stage (C-index = 0.651). Then, the nomogram constructed by combining FAM83A and naive B cells further improved the accuracy of survival prediction.

## Conclusion

The study found that FAM83A has excellent prognostic ability based on various machine learning algorithms. Thus, FAM83A may serve as a potential prognostic marker for NSCLC. Subsequently, we applied the SVM-based CIBERSORT algorithm to assess the immune cell components of the NSCLC microenvironment. We used three machine learning algorithms to identify naive B cells significantly related to the survival of NSCLC patients. In addition, the nomograms of naive B cells and FAM83A better predict the overall survival rate of NSCLC than in the traditional stage. Therefore, the abnormal infiltration of naive B cells associated with FAM83A may be a critical factor in predicting the

prognosis of NSCLC patients. Still, it needs to be further verified by clinical trials.

## Data availability statement

The original contributions presented in the study are included in the article/Supplementary Material. Further inquiries can be directed to the corresponding authors.

## Author contributions

PT wrote the manuscript. ZW designed the study. XL and LC contributed to the data collection. MZ and ZX contributed to data analysis and figure preparation. The authors read and approved the final manuscript.

## Funding

The study was supported by Natural Science Foundation of Xiaogan (Grant Number: XGKJ2021010024).

## References

1. Jonna S, Subramaniam DS. Molecular diagnostics and targeted therapies in non-small cell lung cancer (NSCLC): An update. *Discovery Med* (2019) 27(148):167–70.
2. Imyanitov EN, Iyevleva AG, Levchenko EV. Molecular testing and targeted therapy for non-small cell lung cancer: Current status and perspectives. *Crit Rev Oncol Hematol* (2021) 157:103194. doi: 10.1016/j.critrevonc.2020.103194
3. Naylor EC, Desani JK, et al. Targeted therapy and immunotherapy for lung cancer. *Surg Oncol Clin N Am* (2016) 25(3):601–9. doi: 10.1016/j.soc.2016.02.011
4. Tsoukalas N, Kiakou M, Tsapakidis K, Tolia M, Aravantinou-Fatorou E, Baxevasos P, et al. PD-1 and PD-L1 as immunotherapy targets and biomarkers in non-small cell lung cancer. *J BUON* (2019) 24(3):883–8.
5. Thakur MK, Gadgeel SM. Predictive and prognostic biomarkers in non-small cell lung cancer. *Semin Respir Crit Care Med* (2016) 37(5):760–70.
6. Wang Y, Xu R, Zhang D, Lu T, Yu W, Wo Y, et al. Circ-ZKSCAN1 regulates FAM83A expression and inactivates MAPK signaling by targeting miR-330-5p to promote non-small cell lung cancer progression. *Transl Lung Cancer Res* (2019) 8(6):862–75. doi: 10.21037/tlcr.2019.11.04
7. Lee SY, Meier R, et al. FAM83A confers EGFR-TKI resistance in breast cancer cells and in mice. *J Clin Invest* (2012) 122(9):3211–20. doi: 10.1172/JCI60498
8. Bartel CA, Jackson MW. HER2-positive breast cancer cells expressing elevated FAM83A are sensitive to FAM83A loss. *PLoS One* (2017) 12(5):e0176778. doi: 10.1371/journal.pone.0176778
9. Hu H, Wang F, Wang M, Liu Y, Wu H, Chen X, et al. FAM83A is amplified and promotes tumorigenicity in non-small cell lung cancer via ERK and PI3K/Akt/mTOR pathways. *Int J Med Sci* (2020) 17(6):807–14. doi: 10.7150/ijms.33992
10. Gan J, Li Y, Hu H, Meng Q, Wang F. Systematic analysis of expression profiles and prognostic significance for FAM83 family in non-small-Cell lung cancer. *Front Mol Biosci* (2020) 7:572406. doi: 10.3389/fmolb.2020.572406
11. Xing L, Zhang X, Zhang X, Tong D. Expression scoring of a small-nucleolar-RNA signature identified by machine learning serves as a prognostic predictor for head and neck cancer. *J Cell Physiol* (2020) 235(11):8071–84. doi: 10.1002/jcp.29462

## Conflict of interest

The authors declare that the research was conducted in the absence of any commercial or financial relationships that could be construed as a potential conflict of interest.

## Publisher's note

All claims expressed in this article are solely those of the authors and do not necessarily represent those of their affiliated organizations, or those of the publisher, the editors and the reviewers. Any product that may be evaluated in this article, or claim that may be made by its manufacturer, is not guaranteed or endorsed by the publisher.

## Supplementary material

The Supplementary Material for this article can be found online at: <https://www.frontiersin.org/articles/10.3389/fonc.2022.882018/full#supplementary-material>

12. Newman AM, Liu CL, Green MR, Gentles AJ, Feng W, Xu Y, et al. Robust enumeration of cell subsets from tissue expression profiles. *Nat Methods* (2015) 12(5):453–7. doi: 10.1038/nmeth.3337
13. Tibshirani R. The lasso method for variable selection in the cox model. *Stat Med* (1997) 16(4):385–95. doi: 10.1002/(SICI)1097-0258(19970228)16:4<385::AID-SIM380>3.0.CO;2-3
14. Kursa MB. Robustness of random forest-based gene selection methods. *BMC Bioinf* (2014) 15:8. doi: 10.1186/1471-2105-15-8
15. Wang G, Liu L, Zhang J, Li S, Zhang J, Li S, et al. The analysis of prognosis factor in patients with non-small cell lung cancer receiving pneumonectomy. *J Thorac Dis* (2020) 12(4):1366–73. doi: 10.21037/jtd.2020.02.33
16. Le DT, Durham JN, Smith KN, Wang H, Bartlett BR, Aulakh LK, et al. Mismatch repair deficiency predicts response of solid tumors to PD-1 blockade. *Science* (2017) 357(6349):409–13. doi: 10.1126/science.aan6733
17. Liang W, Cai K, Chen H, Fang W, Fu J, Fu X, et al. Society for translational medicine consensus on postoperative management of EGFR-mutant lung cancer, (2019 Edition). *Transl Lung Cancer Res* (2019) 8(6):1163–73. doi: 10.21037/tlcr.2019.12.14
18. Wu Q, Yu L, Lin X, Zheng Q, Zhang S, Chen D, et al. Combination of serum miRNAs with serum exosomal miRNAs in early diagnosis for non-Small-Cell lung cancer. *Cancer Manag Res* (2020) 12:485–95. doi: 10.2147/CMAR.S232383
19. Zhou M, Chen X, Zhang H, Xia L, Tong X, Zou L, et al. China National medical products administration approval summary: Anlotinib for the treatment of advanced non-small cell lung cancer after two lines of chemotherapy. *Cancer Commun (Lond)* (2019) 39(1):36. doi: 10.1186/s40880-019-0383-7
20. Parameswaran N, Bartel CA, Hernandez-Sanchez W, Miskimen KL, Jackson MW, et al. A FAM83A positive feed-back loop drives survival and tumorigenicity of pancreatic ductal adenocarcinomas. *Sci Rep* (2019) 9(1):13396. doi: 10.1038/s41598-019-49475-5
21. Zheng YW, Li ZH, Lei L, Liu CC, Xu HT. FAM83A promotes lung cancer progression by regulating the wnt and hippo signaling pathways and indicates poor prognosis. *Front Oncol* (2020) 10:180. doi: 10.3389/fonc.2020.00180

22. Zhang J, Sun G, Mei X. Elevated FAM83A expression predicts poorer clinical outcome in lung adenocarcinoma. *Cancer biomark* (2019) 26(3):367–73. doi: 10.3233/CBM-190520
23. Sica A, Larghi P, Mancino A, Rubino L, Porta C, Totaro MG, et al. Macrophage polarization in tumour progression. *Semin Cancer Biol* (2008) 18(5):349–55. doi: 10.1016/j.semcancer.2008.03.004
24. Palaga T, Wongchana W, Kueanjinda P. Notch signaling in macrophages in the context of cancer immunity. *Front Immunol* (2018) 9:652. doi: 10.3389/fimmu.2018.00652
25. Jin R, Liu C, Zheng X, Wang X, Feng H, Li H, et al. Molecular heterogeneity of anti-PD-1/PD-L1 immunotherapy efficacy is correlated with tumor immune microenvironment in East Asian patients with non-small cell lung cancer. *Cancer Biol Med* (2020) 17(3):768–81. doi: 10.20892/j.issn.2095-3941.2020.0121
26. Pardoll DM. The blockade of immune checkpoints in cancer immunotherapy. *Nat Rev Cancer* (2012) 12(4):252–64. doi: 10.1038/nrc3239
27. Kayser G, Schulte-Uentrop L, Siene W, Werner M, Fisch P, Passlick B, et al. Stromal CD4/CD25 positive T-cells are a strong and independent prognostic factor in non-small cell lung cancer patients, especially with adenocarcinomas. *Lung Cancer* (2012) 76(3):445–51. doi: 10.1016/j.lungcan.2012.01.004
28. Muto S, Owada Y, Inoue T, Watanabe Y, Yamaura T, Fukuhara M, et al. Clinical significance of expanded Foxp3(+) helios(-) regulatory T cells in patients with non-small cell lung cancer. *Int J Oncol* (2015) 47(6):2082–90. doi: 10.3892/ijo.2015.3196
29. Guo Z, Liang H, Xu Y, Liu L, Ren X, Zhang S, et al. The role of circulating T follicular helper cells and regulatory cells in non-small cell lung cancer patients. *Scand J Immunol* (2017) 86(2):107–12. doi: 10.1111/sji.12566
30. Ma QY, Huang DY, Zhang HJ, Chen J, Miller W, Chen XF, et al. Function of follicular helper T cell is impaired and correlates with survival time in non-small cell lung cancer. *Int Immunopharmacol* (2016) 41:1–7. doi: 10.1016/j.intimp.2016.10.014
31. Li D, He S. MAGE3 and survivin activated dendritic cell immunotherapy for the treatment of non-small cell lung cancer. *Oncol Lett* (2018) 15(6):8777–83. doi: 10.3892/ol.2018.8362
32. Kargl J, Zhu X, Zhang H, Yang GHY, Friesen TJ, Shipley M, et al. Neutrophil content predicts lymphocyte depletion and anti-PD1 treatment failure in NSCLC. *JCI Insight* (2019) 4(24):e130850. doi: 10.1172/jci.insight.130850
33. Chen J, Tan Y, Sun F, Hou L, Zhang C, Ge T, et al. Single-cell transcriptome and antigen-immunoglobulin analysis reveals the diversity of b cells in non-small cell lung cancer. *Genome Biol* (2020) 21(1):152. doi: 10.1186/s13059-020-02064-6
34. Germain C, Devi-Marulkar P, Knockaert S, Biton J, Kaplon H, Letaïef L, et al. Tertiary lymphoid structure-b cells narrow regulatory T cells impact in lung cancer patients. *Front Immunol* (2021) 12:626776. doi: 10.3389/fimmu.2021.626776
35. Biragyn A, Lee-Chang C, Bodogai M. Generation and identification of tumor-evoked regulatory b cells. *Methods Mol Biol* (2014) 1190:271–89. doi: 10.1007/978-1-4939-1161-5\_19
36. Suarez GM, Ane-Kouri AL, González A, Lorenzo-Luaces P, Neningen E, Salomón EE, et al. Associations among cytokines, EGF and lymphocyte subpopulations in patients diagnosed with advanced lung cancer. *Cancer Immunol Immunother* (2021) 70(6):1735–43. doi: 10.1007/s00262-020-02823-1
37. Shang X, Liu J, Li Z, Lin J, Wang H. A hypothesized TNM staging system based on the number and location of positive lymph nodes may better reflect the prognosis for patients with NSCLC. *BMC Cancer* (2019) 19(1):591. doi: 10.1186/s12885-019-5797-8